Climate Modelling User Group [CMUG]

Deliverable 2.0f

Interim report on progress achieved in WP 5.6: Snow dynamics impacts on temperate/high latitude climate

Centres providing input: IPSL (LSCE)

Version nr.	Date	Status
0.1	August 2024	Input from partners
1.0	9 September 2024	Submitted to ESA

Deliverable 2.0f

Interim report on progress achieved in WP 5.6: Snow dynamics impacts on temperate/high latitude climate

Contents

Interim report on progress achieved in WP 5.6: Snow dynamics impacts on temperate/high latitude climate

1. Purpose and scope of this report

This document is the first Interim report on the work carried out in the WP5.6 study of the CCI-CMUG project. Our study aims to improve the representation of snow cover dynamics in temperate and boreal zones within the IPSL climate model, using the snow cover fraction and snow water equivalent products recently released by the CCI-snow (covering the last four decades), to assess the impact of snow cover dynamics and atmospheric feedback on regional to continental climate.

Snow is a critical cryospheric component of the climate system. Its high albedo gives rise to the positive snow-albedo feedback that amplifies global climate variability and is thought to be a driver of the observed Arctic amplification of the current global warming and the observed amplification of global warming at high latitudes. Widely varying treatments of the vegetation masking of snow in forested areas are suspected to be a major reason for large inter-model variations in the intensity of the snow albedo feedback (Krinner et al., 2018).

In the IPSL climate model, the land surface processes and the interactions with the atmosphere are covered by the ORCHIDEE Land Surface Model (LSM) which includes a snow model (Wang et al., 2013; Charbit et al., in press) able to represent the main physical processes occurring in a snowpack and its evolution according to the boundary conditions at both soil and atmosphere interfaces. Snow-vegetation interactions are not explicitly described, but snow albedo and sublimation depend on the grid vegetation through the specific optical properties and surface roughness of the grid cell. SWE products such as Globsnow (Takala et al., 2011; Luojus et al., 2021) have been used in previous works to evaluate the temporal dynamics of the snowpack, mainly over Siberia (Dantec et al., 2017; Guimberteau et al., 2018). Still, the evaluation has to be extended to the global scale. Furthermore, it is well-known that land cover strongly influences some key processes that drive the evolution of the snowpack, such as lateral transport, melting, refreezing, and sublimation. Therefore, the new snow products from the CCI-Snow project, especially the snow cover extent differentiating ground and viewable fractions, are valuable for improving and calibrating snow models.

Through this project, we will thus investigate how using the CCI-Snow products in combination with the CCI medium/high-resolution land cover products and possibly other datasets, can improve the snow dynamics in the IPSL climate model, mainly through optimizing land cover-specific snow parameters. The methodology that we will develop here, should also apply to other land surface models.

Snow modelling in climate models presents specific issues compared to stand-level modelling relative to the spatial and temporal scales. In a climate model, the size of the grid cell may reach several hundred kilometers, which in general, means heterogeneous landscapes, reliefs and meteorological conditions within the grid. In cold weather, this results in heterogeneous snow coverage, large uncertainties in snowfall estimation and the need to consider the impacts of

vegetation and topography in the modelling. In ORCHIDEE, these interactions are not explicitly accounted for, but they are indirectly represented through the representation of a time-varying Snow Cover Fraction (SCF) dependent on the grid cell snow amount (SWE), and the modelling of the grid cell albedo, key model parameter driving the energy balance and the resulting processes. Given the strong interdependency of SCF, SWE and Albedo, the only snow products are not enough to calibrate all parameterizations. Therefore, we are developing in this project a methodology based on the synergistic use of the three kinds of observations, to improve the modelling of the snowpack dynamics at the global scale, accounting for vegetation impacts, through an improved simulation of the snow albedo and resulting energy and water budgets.

In this report, we present the work performed on the two main tasks defined for this project, which are:

- The analysis of the CCI Snow products, the comparison with modelled variables and the preliminary assessment of their potential to evaluate the ORCHIDEE snow model jointly with other datasets such as albedo and land cover products;
- The use of the CCI Snow products to improve the ORCHIDEE snow parameterizations and better simulate the snowpack dynamics and the snow-atmosphere interactions.

2. ORCHIDEE Land Surface Model

2.1 General description

ORCHIDEE is the continental part of the Earth System Model (ESM) of the Institut Pierre-Simon Laplace (IPSL). In this study, we worked with the ORCHIDEE-V3.0 version. The model simulates the energy and water transfers in the soil-atmosphere continuum and at the surface-atmosphere interface, as well as the carbon and nitrogen cycles and their interactions (Vuichard et al., 2019). Vegetation processes are parameterized for 15 different Plant Functional Types (PFTs) presented in Table 1, related to their phenology, leaf type, physiological activity (e.g. C3/C4 photosynthetic pathways) and climate (Harper et al., 2022). Soil mineral composition is defined at the grid-cell level, based on the 12-classes USDA soil classification. While energy and snow processes are computed at the grid-cell scale (one energy budget for the whole cell), water processes are resolved by accounting for the PFTs present in the grid cell, with a maximum of three soil columns separating bare soil from high (e.g. forests) and low (e.g. grasslands) vegetation. Carbon stocks and fluxes are resolved for each PFT present within the grid cell. Different vertical grids are considered depending on the biogeophysical cycles considered. Soil hydrology and thermics share the same grid consisting of 11 layers from the surface and down to 2 m with a geometrically increasing internode distance. Thermal processes are resolved deeper, up to a maximum depth of 90 m, with 7 additional layers and a number of layers of 18 in the standard version. All thermal and hydrological properties are calculated according to soil composition (mineral, carbon and water components), accounting for soil freezing and snow thermo-hydric processes.

ORCHIDEE can be run at various scales ranging from local to global. For the present study, the model requires the prescription of the atmospheric conditions (air pressure, temperature and humidity, wind speed and incoming radiation), a description of the land surface (fraction of the different PFTs, dominant soil texture) and the initialization of the energy, water, carbon and

nitrogen stocks. These conditions are derived from global datasets (i.e. atmospheric reanalysis, land cover and soil texture classifications) or from stand-level measurements.

PFT1: Bare Soil
PFT2: Tropical Evergreen
PFT3: Tropical Raingreen
PFT4: Temperate Needleleaf Evergreen
PFT5: Temperate Broadleaf Evergreen
PFT6: Temperate Broadleaf Summergreen
PFT7: Boreal Needleleaf Evergreen
PFT8: Boreal Broadleaf Summergreen
PFT9: Boreal Needleleaf Deciduous
PFT10: Temperate Natural Grassland (C3)
PFT11: Natural Grassland (C4)
PFT12: Crops (C3)
PFT13: Crops (C4)
PFT14: Tropical Natural Grassland (C3)
PFT15: Boreal Natural Grassland (C3)

Table 1: The 15 Plant Functional Types used in the ORCHIDEE model to describe vegetation

2.2 ORCHIDEE Snow model

The work performed in WP5.6 aims to use the CCI snow products to improve the modelling of snow dynamics in ORCHIDEE. In our model, the snow processes are represented with a physically-based approach where the main processes driving the temporal evolution of the snowpack such as ageing, compaction, sublimation, melting and refreezing, are represented with a 1D-physical system neglecting the lateral transfers. In the original version of the model (Wang et al., 2013), the snowpack is vertically discretized in 3 layers for which snow temperature, density and liquid water content are prognostic variables. Snow is uniformly distributed over the grid cell regardless of vegetation distribution, and the snow cover fraction (SCF) ranges between 0 and 1 according to the snow amount. SCF is parameterized following the formulation of Niu and Yang (2007) which has been shown to better represent the seasonal variation of the relationship linking snow mass and SCF thanks to its dependence on snow density:

$$SCF = \tanh\left(\frac{Z_{snow}}{2.5 z_{0g} \times \left(\frac{\langle \rho_{snow} \rangle}{\rho_{min}}\right)^{m}}\right) \qquad (1)$$

where ρ_{snow} is the snow density averaged over the total thickness of the snowpack, ρ_{min} is the minimum value of snow density (set to 50 kg m^{-3}), that is the density of fresh snow, z_{0g} is the ground roughness length (set to 0.01 m) and m (set to 1.0 in the present study) is an adjustable parameter.
The energy balance at the snow-atmosphere interface is solved at the model time step (30 mn), mostly driven by the snow albedo, which is a key parameter in the model, dependent on snow age and temperature.

Compared to the earlier version presented by Wang et al. (2013), the albedo scheme has been modified and snow albedo is now computed following the formulation of Chalita and Le Treut (1994):

$$\alpha_{snow} = A_{aged} + B_{dec} exp\left(-\frac{\tau_{snow}}{\tau_{dec}}\right) \quad (2)$$

where A_{aged} represents the albedo of a snow-covered surface after snow ageing (old snow) and B_{dec} is defined so that the sum of A_{aged} and B_{dec} represents the albedo of fresh snow (i.e., maximum snow albedo). τ_{dec} is the time constant of the albedo decay and τ_{snow} is the snow age and is parameterized as follows:

$$\tau_{snow}(t+dt) = \left[\tau_{snow}(t) + \left(1 - \frac{\tau_{snow}}{\tau_{max}}\right) \times dt\right] \times exp\left(-\frac{P_{snow}}{\delta_c}\right) + f_{age} \quad (3)$$

where τ_{max} is the maximum snow age, P_{snow} is the amount of snowfall during the time interval dt and δ_c is the critical value of solid precipitation necessary for reducing the snow age by a factor 1/e. As the ORCHIDEE time step is fixed to 30 mn, the snow age is almost zero in a few time steps. In addition, low surface air temperatures found in arctic regions slow down the metamorphism. This effect is accounted for with the function expressed as:

$$f_{age} = \left[\frac{\left(\tau_{snow}(t) + \left(1 - \frac{\tau_{snow}}{\tau_{max}}\right) \times dt\right) \times exp\left(-\frac{P_{snow}}{\delta_c}\right) - \tau_{snow}(t)}{1 + g_{temp}(T_{surf})}\right] \quad (4)$$

$$g_{temp}(T_{surf}) = \left[\frac{max\,(T_0 - T_{surf},\ 0)}{\omega_1}\right]^{\omega_2} \quad (5)$$

Where ω_1 and ω_2 are tuning constants. The albedo is computed for the visible and near-infrared spectral bands. However, to compute the upward shortwave radiation, an arithmetic mean between the visible and the near-infrared albedo is considered.

Recently, Charbit et al., 2024 (in press) extended this snow scheme to ice sheets and for that purpose, modeled the snow-ice interface and used new datasets to validate the snow mass balance. In this work, they showed the improvements brought to the snow temperature prediction by replacing the 3-layer discretization with a 12-layer one, following Decharme et al., 2016. Therefore, the last and shared version of ORCHIDEE (Trunk version) now includes this updated scheme which has still not been fully validated and calibrated over continental surfaces. Furthermore, the Trunk version uses an updated scheme for the computation of the vegetation albedo which still requires calibration.

Our intent is therefore to benefit from the new CCI-Snow products to revise the calibration of the snow model in the Trunk version (that will be used for the CMIP7 model simulations of the IPCC Assessment Report (AR7)). But, given the strong links between SCF and the albedo grid cell, snow albedo calibration requires the prior calibration of the vegetation albedo which is a priority for the ORCHIDEE team and should be performed in fall 2024. Meanwhile, we have worked on the previous ORCHIDEE-V3 version (Vuichard et al., 2019) to develop the calibration methodology and intend to apply it to the Trunk version by the end of the year.

Besides, parallel works are ongoing in our group on the representation of soil thermics in Arctic ecosystems and the impacts of soil organic carbon on thermal soil properties (Gaillard et al., submitted; Cuynet et al., in preparation). In particular, Cuynet et al., (in preparation) developed new parameterizations including a better interpretation of the soil dataset Soilgrids 2.0 (Poggio et al., 2021), used in ORCHIDEE to prescribe soil properties.

We can note also that the last Trunk version includes new PFT maps derived from the ESA CCI MRLC project (PFT V3.0 product, Harper et al., 2022) which show significant improvements compared to the former ones (Lurton et al., 2021), especially in Arctic areas, where shrublands were overestimated at the expense of grasslands and bare soils (Harper et al., 2022; Ottlé et al., internal reports).
All these developments are now merged in the Trunk version and will benefit our further developments.

3. Progress on the tasks

Two internships have been dedicated to the tasks of WP5.6. Some of the works presented here are direct results of these internships (Guillermo Cossio, summer 2023, and Benoît Lecomte, fall 2023, internal reports).

3.1 Progress on WP5.6.1: CCI-Snow products analysis

3.1.1 Presentation of the Snow CCI products and albedo product

The Snow CCI products (Solberg et al., 2021) provide several global daily time series of essential climate variables (ECV) related to snow:

- Snow Cover Fraction Viewable (SCFV)
- Snow Cover Fraction Ground (SCFG)
- Snow Water Equivalent (SWE)

The SCFV corresponds to snow on top of open areas and vegetation like forest canopies, while the SCFG is the snow on the ground for open land, corrected for masking by trees in forested areas. The snow cover for each grid cell is given as a percentage. The SWE indicates the amount of snow accumulated on land surfaces, as an equivalent height of water.

More details on the products are provided in Table 2.

Moreover, the MODIS daily global albedo product (doi:10.5067/MODIS/MCD43C3.061) is also used in this analysis, since SCF and albedo are interrelated. The MODIS Albedo products MCD43A3 available at a resolution of 0.01° and over the period 2000-2020 was chosen to evaluate the model predictions, analyze model errors and calibrate the model parameters.

	SCFG	SCFV	SWE
Product name	Snow Cover Fraction Ground	Snow Cover Fraction Viewable	Snow Water Equivalent
DOI	10.5285/8847a05eeda646a29da58b42bdf2a87c	10.5285/ebe625b6f77945a68bda0ab7c78dd76b	10.5285/4647cc9ad3c044439d6c643208d3c494
Description	Daily snow cover fraction (0-100%) **on the ground** per pixel for global land areas (excluding pixels containing more than 50% of permanent snow and ice, and pixels containing more than 30% of water)	Daily snow cover fraction (0-100%) **on top of the forest canopy** per pixel for global land areas (excluding pixels containing more than 50% of permanent snow and ice, and pixels containing more than 30% of water)	Daily snow water equivalent (in mm) per pixel, representing the amount of water stored in the snowpack Covers the Northern Hemisphere land areas, excluding mountainous regions, glaciers, and Greenland
Cloud handling	Clouds are masked		Not affected by clouds
Data Source	Medium-resolution optical satellite data		Low-resolution passive microwave satellite data combined with in-situ snow depth measurements
Instrument	MODIS / AVHRR (separate products)		SMMR, SSM/I and SSMIS PMR (merged product)
Spatial resolution	~1 km per pixel for MODIS (coarser resolution for AVHRR)		0.10-degree latitude-longitude grid
Uncertainty	Unbiased Root Mean Square Error (RMSE) per pixel		Statistically derived accuracy estimates on each pixel level
Auxiliary datasets	- **ESA CCI Land Cover 2000**: Masks water bodies and permanent snow/ice (aggregated to the pixel size of SCF product) - **Forest Canopy Transmissivity Map**: Derived from ESA CCI Land Cover 2000 and Landsat tree cover density map (Hansen et al., 2013, DOI: 10.1126/science.1244693) for canopy correction	- **ESA CCI Land Cover 2000**: Masks water bodies and permanent snow/ice (aggregated to the pixel size of SCF product)	- **ESA CCI Land Cover 2000**: Masks water bodies (aggregated to the pixel size of SWE product) - **ETOPO5-based Mountain Mask**: Used to exclude mountainous regions in the Northern Hemisphere (developed for the ESA GlobSnow project)
Other info	Forest canopy correction is applied based on the forest canopy transmissivity map		

Table 2: Snow CCI products description

3.1.2 Comparison of the MODIS SCF and the AVHRR SCF

Snow CCI provides SCF products from different sensors, including MODIS and AVHRR (among others), which were chosen because of their global resolution and the long time series they provide. The SCF values have been compared in a small region and are presented in Figures 1 (SCFV) and 2 (SCFG) with their uncertainties. The patterns are similar, but differences between the two products can be observed. Moreover, the uncertainties provided with AVHRR are superior to those provided with MODIS data. The differences between the MODIS and AVHRR SCF are calculated and shown in Figure 3. The SCFG differences are small, because on the selected date, the ground is entirely covered by snow (SCFG close to 100%), while bigger differences can be noticed between the SCFVs. When considering Figure 4 that shows the most common PFT per pixel on the same area, it is interesting to note that the patterns in the SCFV differences seem to be related both to latitude and to the dominant PFT map. Indeed, in the presence of grasslands or PFT9, MODIS SCFV is below that of AVHRR, while when PFT7 is mostly represented, the MODIS SCFV is bigger. Also, larger differences are observed in the northern part of the domain with a clear threshold around 55°N. These features seem to be related to the different characteristics of MODIS and AVHRR sensors and orbital parameters as well as methods used to correct bi-directional reflectances.

From this preliminary analysis, the choice was made to use the MODIS SCF for data analysis and model optimization, since the resolution is finer and the uncertainties are less important.

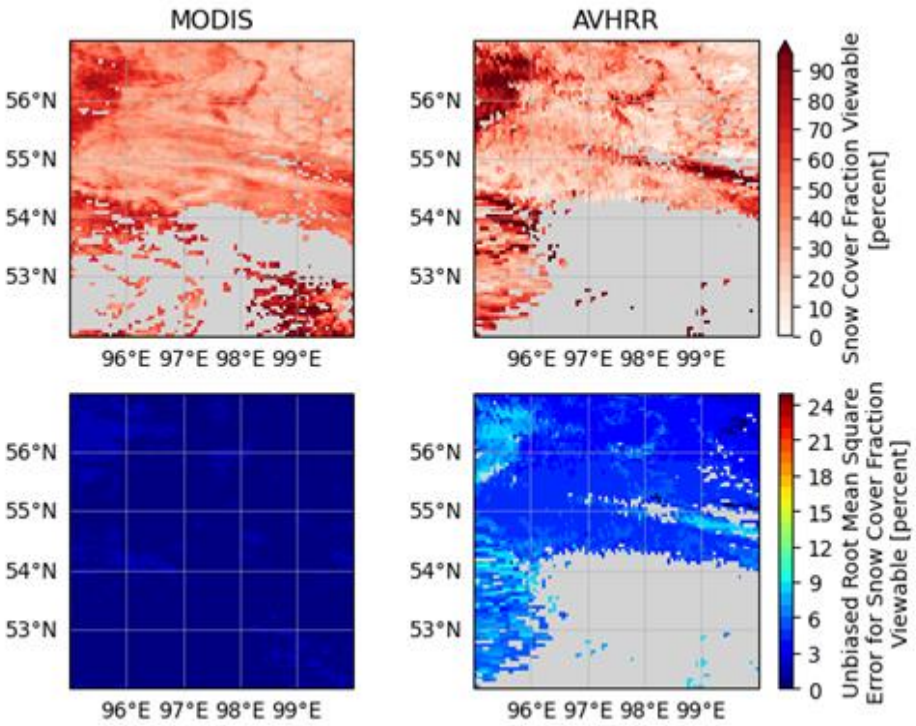

Figure 1: SCFV from MODIS (upper left) and AVHRR (upper right), and the corresponding unbiased RMSE (lower panels) – day: 02/02/2010

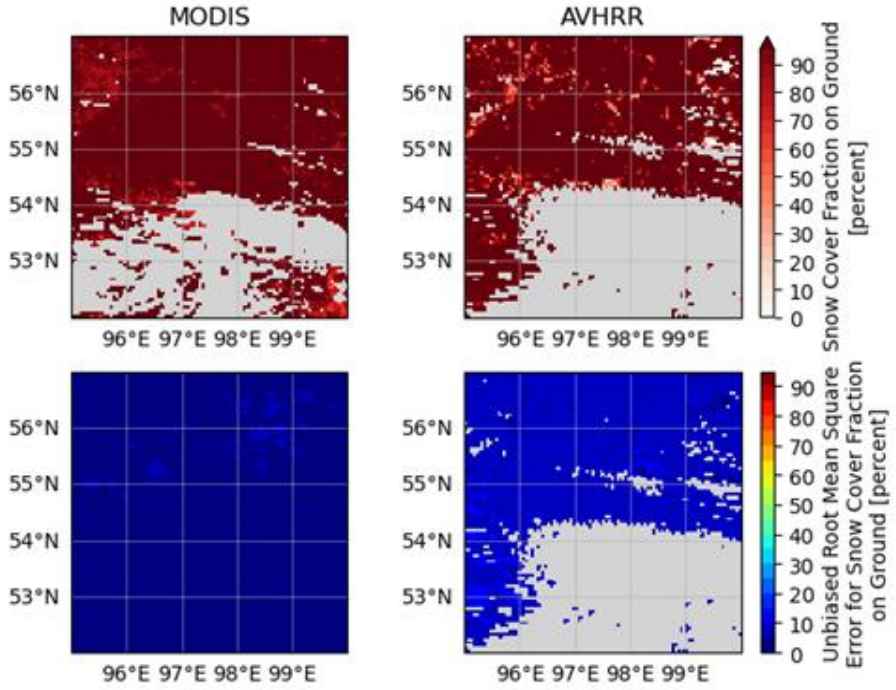

Figure 2: SCFG from MODIS (upper left) and AVHRR (upper right), and the corresponding unbiased RMSE (lower panels) – day: 02/02/2010

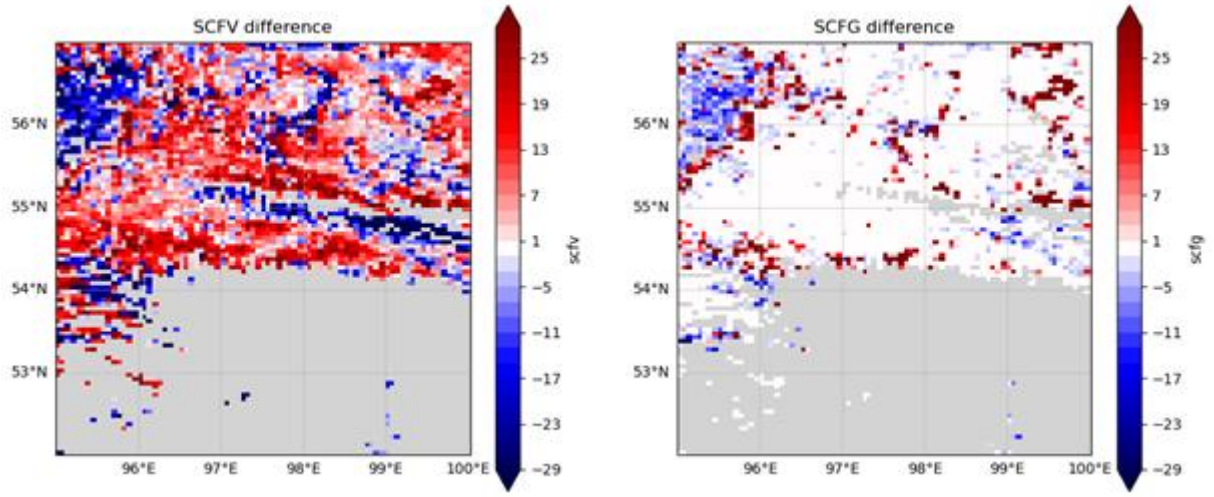

Figure 3: Differences between MODIS and AVHRR SCFV (left) and SCFG (right) – date: 02/02/2010

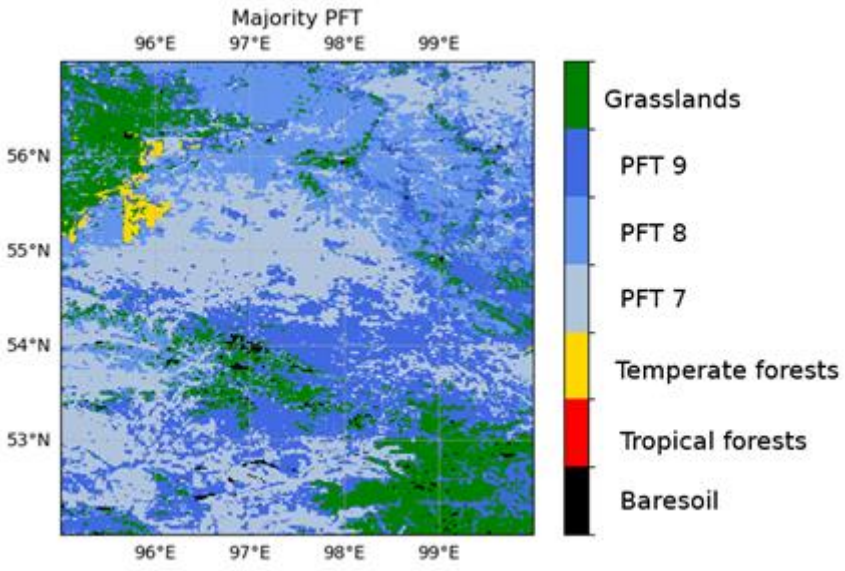

Figure 4: Most common PFT per pixel in the studied region extracted from the ORCHIDEE PFT map derived from the CCI – Medium Resolution Land Cover dataset

3.1.3 Site evolution of SCF and SWE

Time series of SCF and SWE on different sites have been studied. An example is provided in Figure 5, with the evolution of the SCFG, SCFV and SWE, with their uncertainties. The evolution of the different time series is consistent, and uncertainties related to the SCF are not too wide. However, we have noticed rather large uncertainties regarding the SWE, and that was the case on every studied site. The uncertainty may be overestimated, and further attention will be given to that variable in the future, but for the present report, the choice was made to focus mainly on the SCF because of this concern.

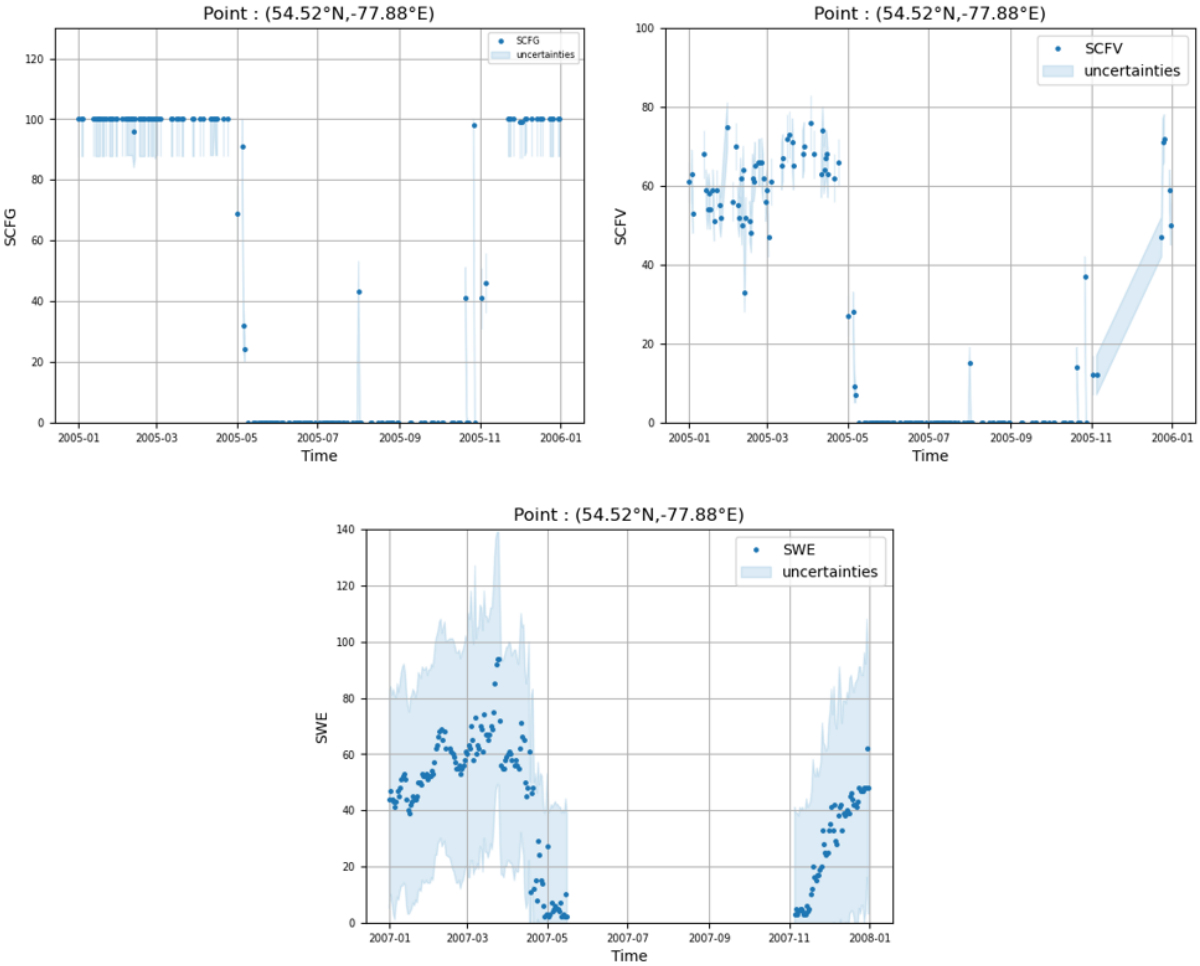

Figure 5: Time series of MODIS SCFG [%], MODIS SCFV [%] and SWE [mm] with the provided uncertainties at a selected point in Siberia (54.52°N, -77.88°E)

3.1.4 Influence of vegetation type on snow dynamics

It is complex to attribute the evolution of the Snow Cover Fraction to the vegetation, because of the huge spatial variability of the meteorological conditions at the scale of the remote sensing products (i.e., a few kilometers at best). It is therefore not possible to compare the results obtained at sites that are too distant from each other since the meteorological conditions may vary widely. A first attempt at identifying the role of the vegetation on the snow behavior was thus made by selecting a small part of a region that was considered to be fairly homogeneous in terms of snowfall and topography.

Therefore, a region of 0.5°×0.5° has been selected in Siberia (latitudes between 55.5 and 56°N, and longitudes between 96.5 and 97°E), which is mainly covered by two PFTs: boreal needleleaf evergreen vegetation (PFT7) and boreal broadleaf summergreen vegetation (PFT8), as seen on the right panel in Figure 6, that indicates the most common PFT on 0.05° large pixels when it represents more than 50% of the area. In this particular region, there are 30 pixels that

mostly contain PFT7, and 25 pixels containing PFT8. To produce the time series appearing in Figure 6, that show the evolution of SCFV and SCFG for both PFTs, a spatial averaging is performed for each day and each PFT. The number of points where data are available vary from one day to another because of the possible presence of clouds, that sometimes prevents the measurement of the SCFs.

Figure 6 shows that the SCFV for PFT7 is lower than for PFT8, while the differences between the SCFG are less important. Based on this first result, the impact of the vegetation on the SCF can already be emphasized.

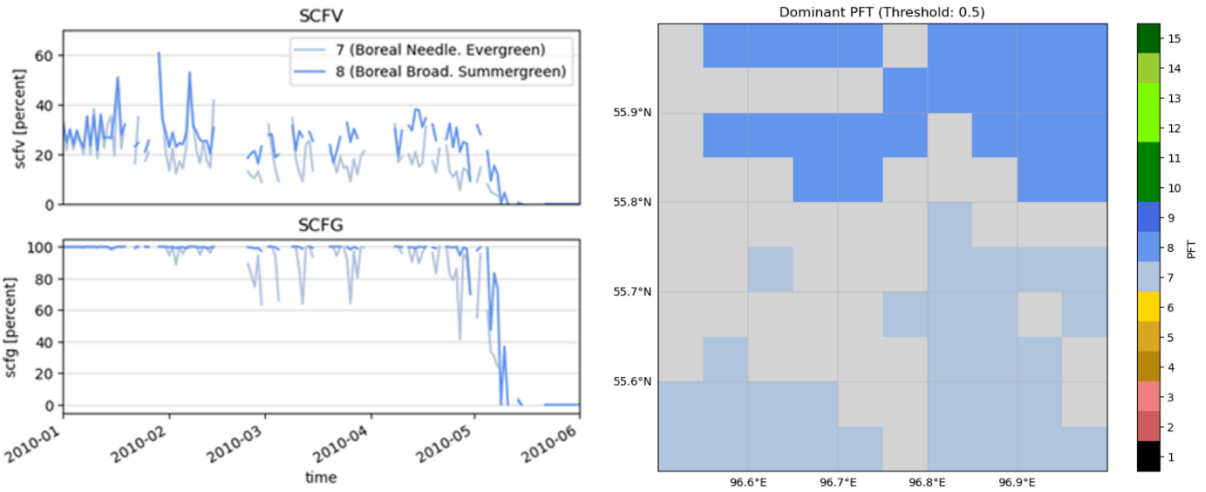

Figure 6:Comparison of the SCFV and SCFG extracted over two types of vegetation (boreal needleleaf evergreen and boreal broadleaf summergreen) in the same region (Siberia) (left), and repartition of the most common PFT in the region derived from the CCI – Medium Resolution Land Cover dataset (right)

3.1.5 Comparison of the SCF and albedo products to ORCHIDEE simulations

Figure 7 shows the difference between the monthly averaged SCF from ORCHIDEE and the CCI Snow SCFG based on the MODIS instruments for each month from December 2010 (upper left panel) to May 2011 (lower right panel). An overestimation during the snow accumulation period is visible, especially in the high latitudes, while the SCFG is underestimated by ORCHIDEE during the ablation period.

Figure 8 provides the albedo differences between ORCHIDEE and the monthly averages from MODIS for the same months. Most of the time, the albedo is underestimated by ORCHIDEE, and in particular during the late months of winter (from March). It can be noted that the SCF differences from Figure 7 and the albedo differences from Figure 8 are consistent. A feedback loop exists between the SCF and the albedo. Indeed, when the albedo is underestimated, it means that the surface absorbs more solar radiation, which may in turn lead to excessive snowmelt, and therefore to lower SWE and SCF, and an even more reduced albedo.

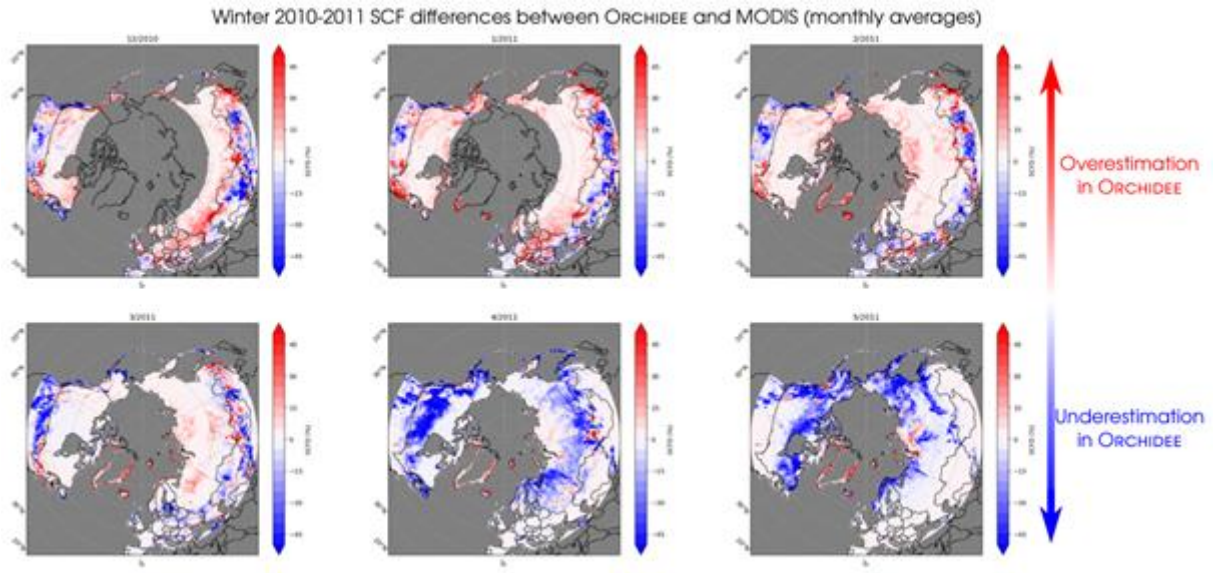

Figure 7: Difference between the SCF calculated in ORCHIDEE and the observed SCF (monthly averages) from December 2010 to May 2011

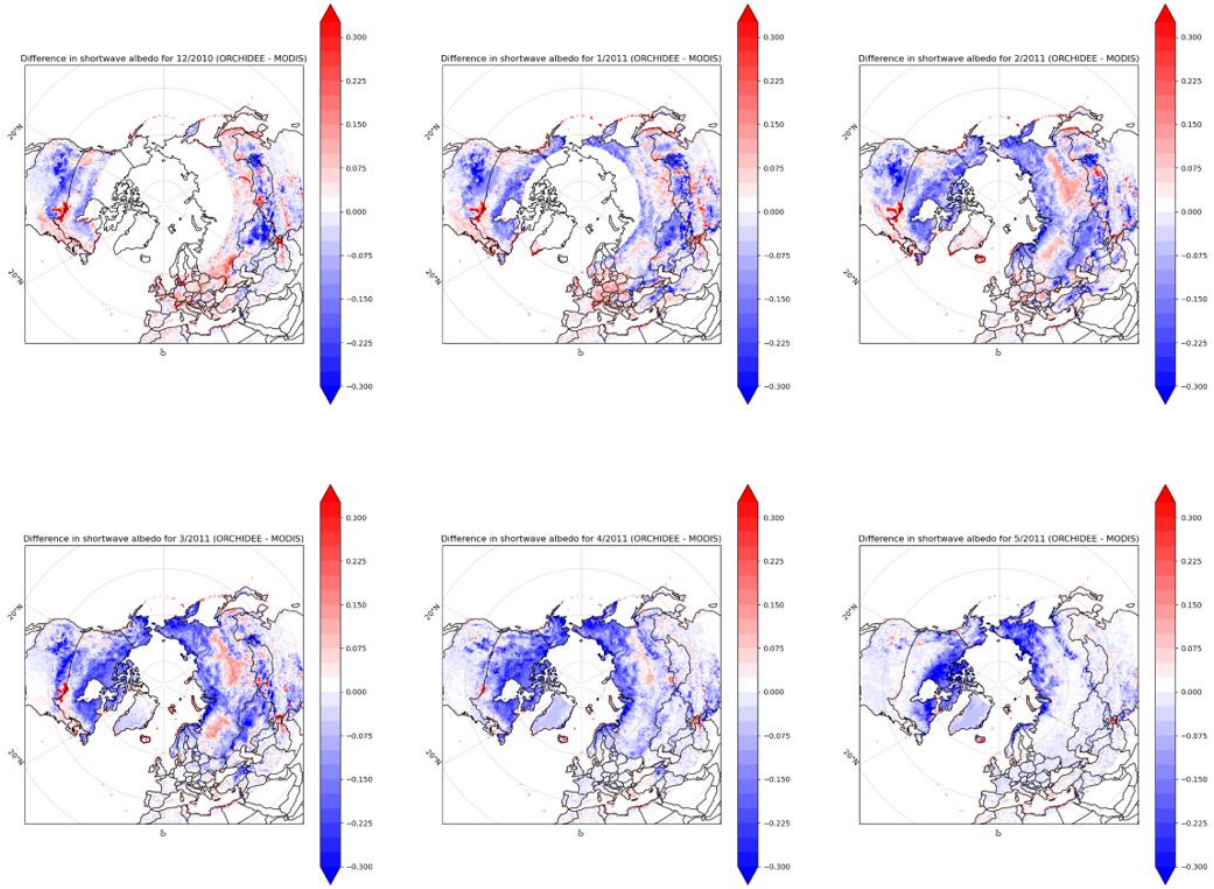

Figure 8: Differences between the albedo computed in ORCHIDEE and the albedo measured by MODIS as monthly averages for Winter 2010-2011

Since both SCF and albedo are related, it is of paramount importance to improve the estimation of both variables in the ORCHIDEE LSM, and in turn, to consider the influence of vegetation which can modify the snow behavior. From this observation, the surface albedo and the snow cover fraction parameterizations both need to be optimized jointly.

3.1.6 Spatial selection of sites for analysis and for model optimization via data assimilation

Since one of the goals of the study is to assess the influence of the vegetation on the snowpack temporal dynamics, it is essential to be able to select sites with homogeneous vegetation. The method developed here relies on the Plant Functional Types map used in the ORCHIDEE LSM, derived from land cover maps.

To select the most suited sites for the analysis, it is necessary to find locations with the highest fraction of the considered PFT. Since the analysis focuses on the retroaction between snow and vegetation, a site of interest would be covered by snow for a long period of time, and data would be available for most days. The selection approach deals with all these aspects.

It is based on the concept of acquisition functions used in Bayesian optimization, which aims to estimate the potential gain in information by exploring a spatial domain. The idea is to assign a score to each point of this domain and then select those with the highest scores.

This score, which is further called the "desirability" of the point, must consider the dominance of the relevant PFT as well as the number of available measurements for days when the pixel is almost completely snow-covered. Additionally, the selection must ensure that the chosen points are not all concentrated in the same region. Therefore, the points are selected sequentially, and each time a point is chosen, the desirability function is updated to reduce the score of points that are close to those already selected.

Mathematically speaking, it means maximizing the desirability function D_i at each iteration i:

$$D_i(x) = V(x) - k\, P_i(x, x_{i-1}, \dots, x_0) \quad (6)$$

Where V is a function of the PFT fraction and the number of days where snow data is available with the SCF of the pixel over a certain threshold, while P_i is a penalty function evaluating the distance d of point x compared to the previous selected points.

$$V(x) = \log(n_{snow}(x)) \times PFT\ fraction(x) \quad (7)$$

$$P_i(x) = \left[\min_{j=0,\dots,i-1} \log\left(1 + d\left(x, x_j\right)\right)\right]^{-1} \quad (8)$$

Taking the logarithm of the distance instead of the distance itself reduces the penalty difference for points that are far from the other selected points, while still maintaining a strong decrease in desirability for points in their vicinity.

3.2 Progress on WP5.6.2: ORCHIDEE model developments

3.2.1 Snow albedo calibration

As explained previously, we have worked with the ORCHIDEE-V3.0 version assuming that the free-snow vegetation albedo parameters are correctly calibrated. Then, the albedo and snow cover products can be used jointly to calibrate the snow model parameters (albedo and SCF). As shown in section 3.1.5, the first task is to revise the snow albedo parameters to remove the overall biases before revising the SCF parameterization.

For that purpose, we used the MODIS Albedo products MCD43A3 available at a resolution of 0.01° and over the period 2000-2020, to evaluate the model predictions, analyze model errors and calibrate the model parameters.

Given that the snow albedo parameters are PFT-dependent, we used the selection process presented in Section 3.1., to select the purest pixels for the dominant vegetation types present in the northern hemisphere, i.e., PFT 4, 5, 6, 7, 8 and 9. As a first step, we worked on the forested PFTs (PFTs 7, 8 and 9) and selected 10 pixels for each PFT for which a significant snow period was present during the 3-year period 2005-2007. We used the calibration algorithm based on a genetic approach (Bastrikov et al., 2018), to calibrate the 2 albedo parameters (snow_aged and snow_dec). The prior and optimized values obtained are given in Table 3.

Before			After		
PFT	Aged	Dec	Aged	Dec	
7	0,18	0,05	0,23	0,044	VIS
8	0,18	0,06	0,14	0,022	
9	0,33	0,09	0,49	0,027	
7	0,16	0,04	0,23	0,016	NIR
8	0,17	0,07	0,14	0,017	
9	0,27	0,08	0,37	0,015	

Table 3: Prior and Posterior values of the two albedo model parameters calibrated against MODIS observations

An example of prior and posterior modeled albedo for two sites and two types of PFT (8 and 9) are given in Figure 9.

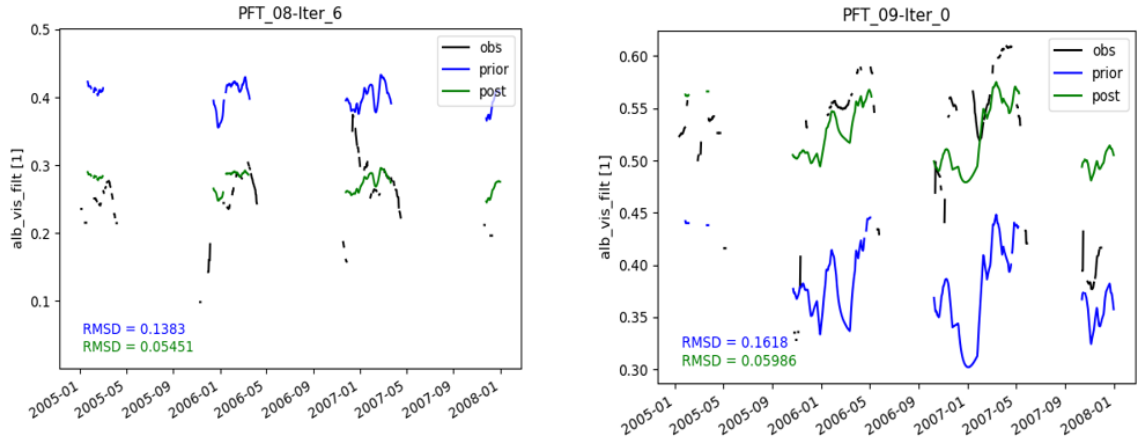

Figure 9: Prior and Posterior albedo values calculated by ORCHIDEE over a 3-year period (2005-2008) for 2 sites covered mainly by PFT 8 (Boreal Broadleaf Summergreen) and PFT 9 (Boreal Deciduous Needleleaf) forest

At larger scale, the new parameters allow to decrease the albedo biases especially in winter but large errors remain during the melting period, reinforcing the need to revise the SCF parameterization in a second step.

3.2.2 SCF model calibration

Once the snow albedo parameters are calibrated, the SCF parameterization can be revised. First, we performed a sensitivity analysis to quantify the sensitivity of the model parameters (Z0, fresh snow density and an additional scaling factor which could be PFT dependent) on the snow-simulated variables (SCF, snow mass, snowmelt and sublimation. For that task, we used the Morris approach which allows to rank the parameter importance, separating the snow accumulation and melting periods, to account for the well-known hysteresis of the relationship linking SWE and SCF.
The results show the varying importance of the parameters between the two seasons (winter and spring), with a larger importance of roughness parameters in spring compared to winter and the PFT dependence larger in winter with impacts differing among the 5 simulated variables (i.e., SCF, SCFV, SWE, snowmelt and sublimation).

Then, we first decided to revise the density of fresh snow which was set to a value of 50kg/m3 which appears too low compared to published values and increased it to a more realistic value of 100kg/m3. In a second step, we performed different assimilation tests to adjust the calibration settings and perform the calibration of the two remaining parameters (scaling factor relative to roughness height and PFT type). In particular, we decided to calibrate the parameters as a first step only on the period where they are sensitive (by selecting the observations used in the cost function) and to perform a final optimization with all parameters and all the observations at the end. Some preliminary results were obtained but some limitations appeared, linked to some albedo biases identified for some PFT classes. They confirmed the need for a prior careful calibration of the free-snow vegetation parameters, before performing the snow model ones. This task will be done in the following months.

4. Summary

The work performed during this first year allowed to progress on the two main tasks of the project which are:
- the analysis of the CCI-Snow products (SCFV, SCFG and SWE) and their preliminary comparison with the ORCHIDEE V3.0 version, and
- the assessment of their potential to improve the modelling of the snow cover fraction and the calibration of the albedo related parameters.

A protocol has been set up to select the most homogeneous pixels at the product spatial resolution for the revision of the model calibration. This methodology has to be applied now to the current trunk version. The next steps will be to update the current trunk version with the new PFT maps developed by Harper et al., 2022, to recalibrate the vegetation albedo parameters, before revising the SCF parameterization and performing a new calibration. All this framework is now set up to use the CCI Snow products and assess their contribution for improving snowpack dynamics modelling in ORCHIDEE and study atmospheric interactions in a second step.

5. References

Bastrikov, V., Macbean, N., Bacour, C., Santaren, D., Kuppel, S. and Peylin, P.: Land surface model parameter optimisation using in situ flux data: Comparison of gradient-based versus random search algorithms (a case study using ORCHIDEE v1.9.5.2), *Geosci. Model Dev., 11(12),* 4739–4754, doi:10.5194/gmd-11-4739-2018, 2018.

Boone, A., and Etchevers, P.: An intercomparison of three snow schemes of varying complexity coupled to the same land surface model: Local-scale evaluation at an Alpine site. *Journal of Hydrometeorology, 2(4),* 374-394, 2001.

Cheruy, F., Ducharne, A., Hourdin, F., Musat, I., Vignon, É., Gastineau, G., et al.: Improved near-surface continental climate in IPSL-CM6A-LR by combined evolutions of atmospheric and land surface physics, *Journal of Advances in Modeling Earth Systems, 12*, e2019MS002005., doi: 10.1029/2019MS002005, 2020.

Cuynet, A., Salmon, E., Ottlé, C.: Enhanced prescription of soil organic and mineral content in the ORCHIDEE LSM to determine soil thermal properties: implications for northern high latitude sites, in preparation.

Dantec-Nédélec, S., Ottlé, C., Wang, T., Guglielmo, F., Maignan, F., Delbart, N., ... & Jouzel, J. (2017). Testing the capability of ORCHIDEE land surface model to simulate A rctic ecosystems: Sensitivity analysis and site-level model calibration. *Journal of Advances in Modeling Earth Systems*, *9*(2), 1212-1230.

Decharme, B., Brun, E., Boone, A., Delire, C., Le Moigne, P. and Morin., S.: Impacts of snow and organic soils parameterization on northern Eurasian soil temperature profiles simulated by the ISBA land surface model, *The Cryosphere, 10*, 853-877, doi: 10.5194/tc-10-853-2016, 2016.

Chalita, S. and Le Treut, H.: The albedo of temperate and boreal forest and the Northern Hemisphere climate: a sensitivity experiment using the LMD GCM, *Climate Dynamics, 10*, 231-240, doi: 10.1007/BF00208990, 1994.

Charbit S., Ch. Dumas, F. Maignan, C. Ottlé, N. Raoult, X. Fettweis and P. Conesa: Modelling snowpack on ice surfaces with the ORCHIDEE land surface model: Application to the Greenland ice sheet. *The Cryosphere*, in press.

Gaillard, R., Peylin, P., Cadule, P., Bastrikov, V., Cheruy, F., Cuynet, A., Ghattas, J., Zhu, D., Guenet, B. Arctic soil carbon insulation averts large spring cooling from surface-atmosphere feedbacks. Submitted to *Proceedings of the National Academy of Sciences (PNAS).*

Guimberteau, M., Zhu, D., Maignan, F., Huang, Y., Yue, C., Dantec-Nédélec, S., ... & Ciais, P. (2018). ORCHIDEE-MICT (v8. 4.1), a land surface model for the high latitudes: model description and validation. *Geoscientific Model Development*, *11*(1), 121-163.

Harper, K. L., Lamarche, C., Hartley, A., Peylin, P., Ottlé, C., Bastrikov, V., ... & Defourny, P. (2023). A 29-year time series of annual 300 m resolution plant-functional-type maps for climate models. *Earth System Science Data*, *15*(3), 1465-1499.

Hourdin, F., Musat, I., Bony, S., Braconnot, P., Codron, F., Dufresne, J., Fairhead, L., Filiberti, M., Friedlingstein, P., Grandpeix, J., Krinner, G., Le Van, P., Li, Z.-X., and Lott, F.: The LMDZ4 general circulation model: climate performance and sensitivity to parametrised physics with emphasis on tropical convection, *Climate Dynamics*, *27*, 787–813, doi:10.1007/s00382-006-0158-0, 2006.

Krinner, G., Viovy, N., de Noblet-Ducoudré, N., Ogée, J., Polcher, J., Friedlingstein, P., Ciais, P., Sitch, S., and Prentice, I. C.: A dynamic global vegetation model for studies of the coupled atmosphere-biosphere system, *Global Biogeochemical Cycles*, *19*, GB1015, doi:10.1029/2003GB002199, 2005.

Luojus, K., Pulliainen, J., Takala, M., Lemmetyinen, J., Mortimer, C., Derksen, C., ... & Venäläinen, P. (2021). GlobSnow v3. 0 Northern Hemisphere snow water equivalent dataset. *Scientific Data*, *8*(1), 163.

Lurton, T., Balkanski, Y., Bastrikov, V., Bekki, S., Bopp, L., Braconnot, P., ... & Boucher, O. (2020). Implementation of the CMIP6 Forcing Data in the IPSL-CM6A-LR Model. *Journal of Advances in Modeling Earth Systems*, *12*(4), e2019MS001940.

Niu, G.-Y., and Yang, Z.-L.: An observation-based formulation of snow cover fraction and its evaluation over large North American river basins, *Journal of Geophysical Research*, *112*, D21101, doi:10.1029/2007JD008674, 2007.

Poggio, L., De Sousa, L. M., Batjes, N. H., Heuvelink, G. B., Kempen, B., Ribeiro, E., & Rossiter, D.: SoilGrids 2.0: producing soil information for the globe with quantified spatial uncertainty. *Soil, 7(1)*, 217-240, https://doi.org/10.5194/soil-7-217-2021, 2021.

Raoult, N., Charbit, S., Dumas, C., Maignan, F., Ottlé, C., and Bastrikov, V.: Improving modelled albedo over the Greenland ice sheet through parameter optimisation and MODIS snow albedo retrievals, *The Cryosphere, 17*, 2705–2724, https://doi.org/10.5194/tc-17-2705-2023, 2023.

Solberg, R., G. Schwaizer, T. Nagler, S. Wunderle, K. Naegeli, K. Luojus, M. Takala, J. Pulliainen, J. Lemmetyinen, and M. Moisander: ESA CCI+ Snow ECV: Product User Guide, version 3.1, December 2021, 2021.

Takala,M., Luojus, K., Pulliainen, J., Derksen, C., Lemmetyinen, J., Kärnä, J.-P., Koskinen, J. and Bojkov, B., 2011. Estimating northern hemisphere snow water equivalent for climate research through assimilation of space-borne radiometer data and ground-based measurements, *Remote Sensing of Environment, Volume 115, Issue 12*, 15 December 2011, Pages 3517-3529. doi: 10.1016/j.rse.2011.08.014

Vuichard, N., Messina, P., Luyssaert, S., Guenet, B., Zaehle, S., Ghattas, J., Bastrikov, V. and Peylin, P.: Accounting for carbon and nitrogen interactions in the global terrestrial ecosystem model ORCHIDEE (trunk version, rev 4999): Multi-scale evaluation of gross primary production. *Geoscientific Model Development, 12(11)*, 4751-4779, doi:10.5194/gmd-12-4751-2019, 2019.

Wang, T., Ottlé, C., Boone, A., Ciais, P., Brun, E., Morin, S., Krinner, G., Piao, S. and Peng, S.: Evaluation of an improved intermediate complexity snow scheme in the ORCHIDEE land surface

model, *Journal of Geophysical Research Atmosphere, 118*, 6064–6079, doi:10.1002/jgrd.50395, 2013.

Wang, T., Peng, S., Krinner, G., Ryder, J., Li, Y., Dantec-Nédélec, S. and Ottlé, C.: Impacts of Satellite-Based Snow Albedo Assimilation on Offline and Coupled Land Surface Model Simulations. *PLoS ONE 10(9):* e0137275, doi:10.1371/journal.pone.0137275, 2015.

6. Glossary

Terms	
Data assimilation	Observations directly influence the model initial state taking into account their error characteristics during every cycle of a model. This is used for reanalysis, NWP, which includes seasonal and decadal forecasting.
Model validation	Observations are compared with equivalent model fields to assess the accuracy of the model. This can be on short time scales for process studies or long time scales for climate trends.
Climate monitoring	This describes the use of a satellite only dataset to monitor a particular atmospheric or surface variable over a period > 15yrs to investigate whether there is a trend due to climate change.
Initialisation	To initialise prognostic quantities of the model with reasonable values at the beginning of the simulation but do not continuously update.
Prescribe boundary conditions	Prescribe boundary conditions for a model run for variables that are not prognostic (e.g. land cover, ice caps etc).
Accuracy	Accuracy is the measure of the non-random, systematic error, or bias, that defines the offset between the measured value and the true value that constitutes the SI absolute standard.
Stability	Stability is a term often invoked with respect to long-term records when no absolute standard is available to quantitatively establish the systematic error – the bias defining the time-dependent (or instrument-dependent) difference between the observed quantity and the true value.
Precision	Precision is the measure of reproducibility or repeatability of the measurement without reference to an international standard so that precision is a measure of the random and not the systematic error. Suitable averaging of the random error can improve the precision of the measurement but does not establish the systematic error of the observation.
Acronyms	
AVHRR	Advanced Very High Resolution Radiometer
CCI	Climate Change Initiative
CMC	Climate Modelling Community
CMIP6/7	Climate Model Intercomparison Project-6/7
CMUG	Climate Modelling Users Group
ECV	Essential Climate Variable
EGU	European Geophysical Union
ENSO	El Nino- Southern Oscillation
ERA	ECMWF Reanalysis

IPCC	International Panel for Climate Change
LAI	Leaf Area Index
SCF	Snow Cover Fraction
SCFG	Snow Cover Fraction Ground
SCFV	Snow Cover Fraction Viewable
SWE	Snow Water Equivalent